J Low Temp Phys
DOI 10.1007/s10909-016-1483-2

Analysis of Electronic and Structural Properties of Surfaces and Interfaces Based on $LaAlO_3$ and $SrTiO_3$

I. I. Piyanzina[1,2] · Yu. V. Lysogorskiy[1] · I. I. Varlamova[1] · A. G. Kiiamov[1] · T. Kopp[2] · V. Eyert[3] · O. V. Nedopekin[1] · D. A. Tayurskii[1]

Received: 4 July 2015 / Accepted: 4 January 2016

Abstract Recently, it was established that a two-dimensional electron system can arise at the interface between two oxide insulators $LaAlO_3$ and $SrTiO_3$. This paradigmatic example exhibits metallic behaviors and magnetic properties between non-magnetic and insulating oxides. Despite a huge amount of theoretical and experimental work a thorough understanding is yet to be achieved. We analyzed the structural deformations of a $LaAlO_3$ (001) slab induced by hydrogen adatoms and oxygen vacancies at its surface by means of density functional theory. Moreover, we investigated the influence of surface reconstruction on the density of states and determined the change of the local density of states at the Fermi level with increasing distance from the surface for bare $LaAlO_3$ and for a conducting $LaAlO_3/SrTiO_3$ interface. In addition, the Al-atom displacements and distortions of the TiO_6-octahedra were estimated.

Keywords Surface · Interface · LAO/STO · Defects · Density functional · Electronic structure

1 Introduction

Since the discovery of high temperature superconductivity [1] considerable effort has been made to study the behavior of strongly correlated electrons in transition metal oxides. Various types of impurities, crystal structure defects, stoichiometric varia-

✉ I. I. Piyanzina
irina.piyanzina@physik.uniaugsburg.de

1 Institute of Physics, Kazan Federal University, Kremlyovskaya St. 18, Kazan, Russia 420008

2 EP VI and Center for Electronic Correlations and Magnetism, Universität Augsburg, Universitätsstraße 1, 86135 Augsburg, Germany

3 Materials Design SARL, 18 rue de Saisset, 92120 Montrouge, France

Published online: 19 January 2016

tions, external electric and magnetic fields, light illuminations, uniaxial or hydrostatic pressures are accessible parameters for the transition metal oxide properties of films and heterostructures. The structural tuning of films results in a variety of fascinating many-body phenomena.

In particular, the paradigm example of a heterostructure between the non-magnetic and insulating oxides $LaAlO_3$ (LAO) and $SrTiO_3$ (STO) demonstrates rich physics including the coexistence of superconducting 2D electron liquid [2–5] and magnetism [5–11].

The aim of the present study is to investigate the electronic properties and structural distortions of surfaces and interfaces based on LAO and STO by means of density functional theory.

2 Method

We performed ab-initio calculations within density functional theory (DFT) [12,13] and the Vienna Ab-Initio Simulation Package (VASP 5.3) [14] implemented into MedeA software [15]. Exchange and correlation were included at the level of the generalized gradient approximation (GGA) [13]. We have used the projector-augmented wave method [16,17] with a plane-wave basis set and a cutoff energy of 400 eV. The force tolerance was 0.05 eV/Å and the energy tolerance for the self-consistency loop was equal to 10^{-5} eV. The Brillouin zone was sampled on a grid of $5\times5\times1$ **k**-points ($7\times7\times1$ for 4 LAO/4.5 STO/4 LAO heterostructure). In order to avoid the interaction of surfaces and slabs with their periodic images during simulation, a 20 Å vacuum region perpendicular to the surface was added.

3 Results and Discussions

3.1 Surface Properties of LAO and STO

We considered the electronic structure of an LAO (001) slab that consisted of 5.5 unit cells with identical terminations on both sides ($La^{+3}O^{-2}$ or $Al^{+3}O_2^{-2}$). The central region of 1.5 unit cells was kept fixed during the optimization as in Ref. [18]. It was shown in Ref. [19,20] that the surface reconstruction affects intrinsic transport properties of the slab. Since the $La^{+3}O^{-2}$ layers have a charge of +1 and $Al^{+3}O_2^{-2}$ layers have a charge of -1 per unit cell, the unreconstructed (1×1) LaO-terminated (001) surface lacks one electron, whereas the AlO_2-terminated surface has an excess of one electron. We confirmed that the LAO surface with AlO_2-termination has lower energy per area and we will therefore focus on this structure in the discussion below.

Under experimental conditions, thin films of LAO are grown on top of the STO substrate. The lattice constant a of LAO approaches the in-plane lattice parameter a of STO [2],therefore the LAO lattice parameter was fixed at this value ($a = 3.941$ Å from our GGA calculation for bulk STO). It follows from our findings (see Fig. 1) that the bare LAO surface with AlO_2-termination is a semiconductor with a very small gap separating the bulk bands and a narrow surface level.

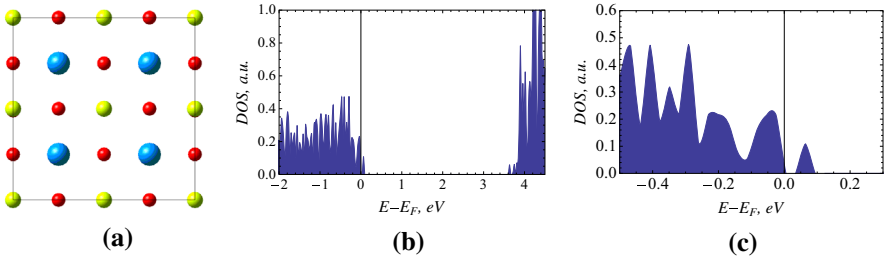

Fig. 1 Top view of an optimized (2×2) bare $LaAlO_3$ (001) surface with AlO_2-termination (**a**), corresponding density of states (DOS) profile (**b**) and its enlarged version near the Fermi level (**c**). *Red spheres* denote oxygen, *blue spheres* denote lanthanum and *yellow spheres* denote aluminum (Color figure online)

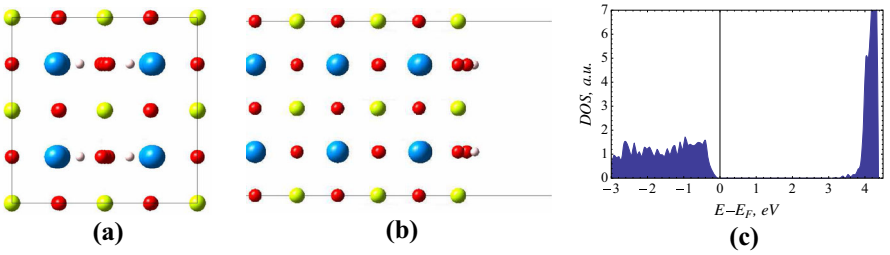

Fig. 2 Top (**a**) and side (**b**) view of an optimized (2×2) $LaAlO_3$ (001) surface with AlO_2-termination and H-adatoms with corresponding density of states (**c**). *Red spheres* denote oxygen, *blue spheres* denote lanthanum and *yellow spheres* denote aluminum, and *white spheres* denote hydrogen (Color figure online)

It is known that the presence of impurities on the surface affects the final termination layer of LAO during surface growth [21]. We considered the case of a hydrogen (H) adatom which is present in almost all growth and annealing environments. The top view of the optimized (2 × 2) $LaAlO_3$ surface with H-adatom at the surface and corresponding DOS are shown in Fig. 2. As in the work of Krishnaswamy et al. [18] the H-adatom bonds to oxygen. It takes a position between the strontium and oxygen and is located above the surface plane. Comparing Figs. 1b, c and 2c it follows that the presence of a H-adatom leads to a filling of the empty states right above the Fermi level of pure LAO and, therefore, a suppression of the albeit small surface conductivity.

The second type of surface reconstruction is caused by an oxygen (O) vacancy. This type is one of the most studied [10,22–25]. For this type of reconstruction we took a (2×2) cell (Fig. 3). As in the case of H-adatoms we obtained a suppression of surface conductivity (Fig. 3c). We performed the same calculations for an STO slab and in contrast to LAO, the STO surface did not show empty states just above the Fermi level and exhibited the same insulator behavior as the bulk STO.

3.2 LAO/STO/LAO Heterostructure Properties

The heterostructures in our calculations consisted of a central region of $SrTiO_3$ (with fixed number of layers $N_{STO} = 4.5$) bounded on both sides with a varying number of $LaAlO_3$ layers (see Fig. 4). According to experimental evidence [2,4], the *n*-type

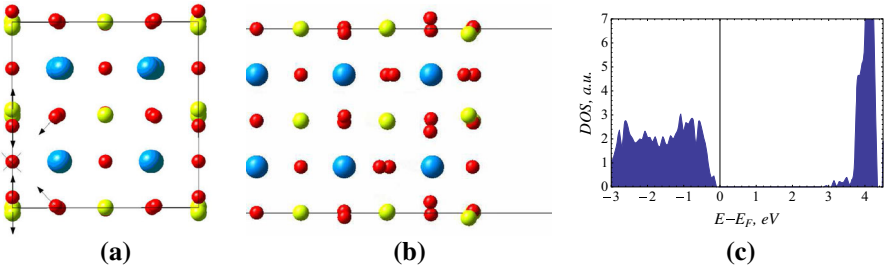

Fig. 3 Top (**a**) and side (**b**) view of an optimized (2×1) $LaAlO_3$ (001) surface with AlO_2-termination and O-vacancy with corresponding density of states (**c**). *Red spheres* denote oxygen, *blue spheres* denote lanthanum, *yellow spheres* denote aluminum, × indicates the oxygen vacancy, and *arrows* point the atoms displacement (Color figure online)

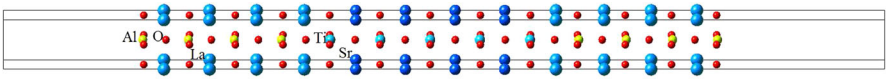

Fig. 4 Structure of 4 LAO/4.5 STO/4 LAO superlattice (Color figure online)

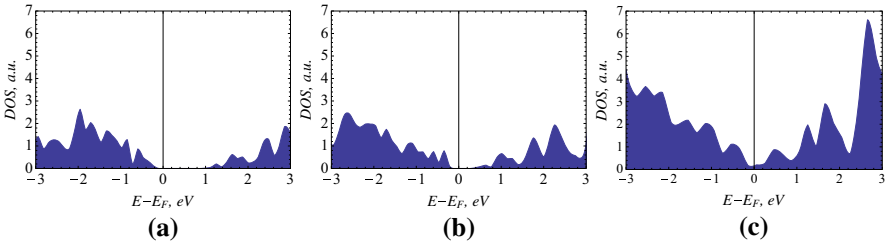

Fig. 5 Density of states plots for LAO/4.5 STO/LAO superlattice interface with (**a**) 2 LAO layers, (**b**) 3 LAO layers, (**c**) 4 LAO layers (Color figure online)

contact with $(TiO_2)^0$–$(LaO)^+$ shows conductivity at the interface and, therefore, we have focused on this type of interface.

We calculated the density of states profiles for a varying number of LAO layers (Fig. 5a–c). It was found that the band gap decreases with an increase in the number of LAO layers. At four LAO layers, the band gap of the LAO/STO/LAO heterostructure vanishes (in agreement with [26]). Layer resolved analysis of the density of states, and structural deformation was performed for this system (Fig. 6).

Figure 6a presents the spatially resolved DOS at the Fermi level $n(E_F)$ of a 4 LAO/4.5 STO/4 LAO heterostructure. The maximum intensity corresponds to surface AlO_2 and the TiO_2 layers on the interface and agrees well with previous findings [2, 10,27]. The value of $n(E_F)$ does not vanish in the middle of the STO slab due to its small thickness during simulations. Orbital decomposition of DOS indicates that the electronic states at the Fermi level consist entirely of Ti $3d_{xy}$ states, which agrees with previous work [10,11,27]. As in the case of a bare LAO surface with AlO_2 termination, there is a contribution to $n(E_F)$ from the surface layers.

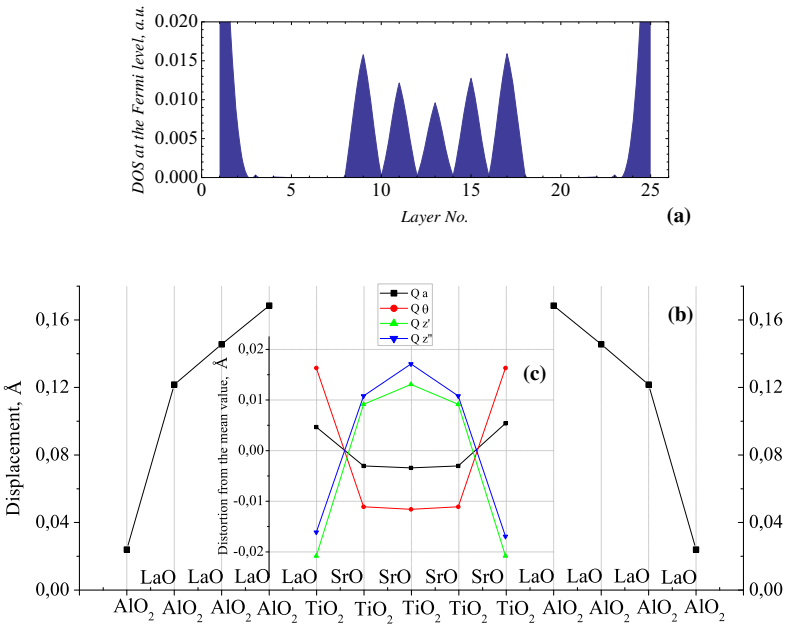

Fig. 6 Projection onto the different layers of 4 LAO/4.5 STO/4 LAO superlattice: density of state at the Fermi level calculated in a small energy window (40 meV) (**a**), displacement of Al atoms with respect to oxygen plane (**b**) and symmetrized displacements Q (normal coordinates) of TiO_6 octahedral systems [28](**c**) (Color figure online)

As a result of the DFT structural optimization, we obtained distortions of the LAO/STO heterostructure, see Fig. 4. Ti atoms moved toward the center of the slab, whereas La atoms shifted toward the surface. Figure 6b shows the displacement of Al atoms out of the oxygen planes. The biggest shift was obtained for Al atoms near the LAO/STO interface. The symmetrized displacements, Q, (normal coordinates) of TiO_6 octahedral system are presented in Fig. 6c. Q_i indicates the collective atom displacements, which, under the symmetry operation, transform according to one of its irreducible representations [28]. The smallest magnitude was found for Q_a breathing mode, which corresponds to a totally symmetric shifting of O atoms out of the center Ti atom. Further non-zero normal coordinates, Q, were associated with oxygen movements in z direction perpendicular to the interface, and they led to the splitting of t_{2g} orbital.

4 Conclusion

In the present work, by means of DFT calculations on the GGA level of theory, we have investigated the structural and electronic properties of the surfaces and interfaces based on the two insulators, LAO and STO. We found that the bare surface of LAO with AlO_2-termination has conductive surface layers, whereas the STO surface is insulating. Two considered types of surface defects (H-adatom and O-vacancy) of the

AlO_2-terminated (001) LAO slab lead to a suppression of surface conductivity. For the LAO/STO/LAO interface, an insulator-metal transition was found by increasing the number of LAO layers from three to four. The largest contribution to the interface conductivity is from the TiO_2 layers (Ti d_{xy} state), decreasing with distance from the interface. We also obtained surface conductivity, which we expect to be suppressed by defects as for the case of the LAO slab.

Acknowledgments The reported study was supported by the Supercomputing Center of Lomonosov Moscow State University with support of the Russian Government Program of Competitive Growth of Kazan Federal University and of the DFG Sonderforschungsbereich TRR 80. The work of A.G. Kiiamov was funded by the subsidy allocated to Kazan Federal University for the state assignment in the sphere of scientific activities. The authors acknowledge helpful discussion with D. Juraschek, A. Petrova, Kate Reidy and Jessica Weitbretch.

References

1. J.G. Bednorz, K.A. Müller, Z. Phys. B **64**, 189 (1986)
2. A. Ohtomo, H. Hwang, Nature **427**, 423 (2004)
3. N. Reyren, S. Thiel, A.D. Caviglia, L.F. Kourkoutis, G. Hammerl, C. Richter, C.W. Schneider, T. Kopp, A.-S. Rüetschi, D. Jaccard, M. Gabay, D.A. Muller, J.-M. Triscone, J. Mannhart, Science **317**, 1196 (2007)
4. S. Thiel, G. Hammerl, A. Schmehl, C. Schneider, J. Mannhart, Science **313**, 1942 (2006)
5. Y. Yu, A. Zunger, Nat. Commun. **5**, 5118 (2014)
6. A. Brinkman, M. Huijben, M. Van Zalk, J. Huijben, U. Zeitler, J. Maan, W. Van der Wiel, G. Rijnders, D. Blank, H. Hilgenkamp, Nat. Mater. **6**, 493 (2007)
7. L. Li, C. Richter, J. Mannhart, R. Ashoori, Nat. Phys. **7**, 762 (2011)
8. Ariando, X. Wang, G. Baskaran, Z.Q. Liu, J. Huijben, J.B. Yi, A. Annadi, A.R. Barman, A. Rusydi, S. Dhar, Y.P. Feng, J. Ding, H. Hilgenkamp, T. Venkatesan, Nat. Commun. **2**, 188 (2011)
9. B. Kalisky, J.A. Bert, B.B. Klopfer, C. Bell, H.K. Sato, M. Hosoda, Y. Hikita, H.Y. Hwang, K.A. Moler, Nat. Commun. **3**, 922 (2012)
10. N. Pavlenko, T. Kopp, E. Tsymbal, J. Mannhart, G. Sawatzky, Phys. Rev. B **86**, 064431 (2012)
11. N. Pavlenko, T. Kopp, J. Mannhart, Phys. Rev. B **88**, 201104 (2013)
12. P. Hohenberg, W. Kohn, Phys. Rev. **136**, B864 (1964)
13. J.P. Perdew, K. Burke, M. Ernzerhof, Phys. Rev. Lett. **77**, 3865 (1996)
14. G. Kresse, J. Furthmüller, Phys. Rev. B **54**, 169 (1996)
15. MedeA®-2.17, Materials Design Inc, Angel Fire, NM, USA, 2015
16. P.E. Blöchl, Phys. Rev. B **50**, 17953 (1994)
17. G. Kresse, D. Joubert, Phys. Rev. B **59**, 1758 (1999)
18. K. Krishnaswamy, C. Dreyer, A. Janotti, C. Van de Walle, Phys. Rev. B **90**, 235436 (2014)
19. A. Janotti, L. Bjaalie, L. Gordon, C. Van de Walle, Phys. Rev. B **86**, 241108 (2012)
20. Y. Xie, Y. Hikita, C. Bell, H.Y. Hwang, Nat. Commun. **2**, 494 (2011)
21. J. Yao, P. Merrill, S. Perry, D. Marton, J. Rabalais, J. Chem. Phys. **108**, 1645 (1998)
22. A. Kalabukhov, R. Gunnarsson, J. Börjesson, E. Olsson, T. Claeson, D. Winkler, Phys. Rev. B **75**, 121404 (2007)
23. V. Vonk, J. Huijben, D. Kukuruznyak, A. Stierle, H. Hilgenkamp, A. Brinkman, S. Harkema, Phys. Rev. B **85**, 045401 (2012)
24. Y. Li, S.N. Phattalung, S. Limpijumnong, J. Kim, J. Yu, Phys. Rev. B **84**, 245307 (2011)
25. L. Zhang, X.F. Zhou, H.T. Wang, J.J. Xu, J. Li, E. Wang, S.H. Wei, Phys. Rev. B **82**, 125412 (2010)
26. F. Cossu, U. Schwingenschlögl, V. Eyert, Phys. Rev. B **88**, 045119 (2013)
27. R. Pentcheva, W.E. Pickett, Phys. Rev. B **74**, 035112 (2006)
28. I.B. Bersuker, *The Jahn–Teller Effect* (Cambridge University Press, Cambridge, 2006)